Network Science **4** (2): 244–265, 2016.
doi:10.1017/nws.2016.5

Interplay between signaling network design and swarm dynamics

ANDRÉ SEKUNDA*
Aalborg University, Fredrik Bajers Vej 5, 9220 Aalborg Ø, Denmark
(e-mail: aksek@elektro.dtu.dk*)*

MOHAMMAD KOMAREJI†
SUTD–MIT International Design Centre, Singapore University of Technology and Design, 8 Somapah Road, 487372, Singapore
(e-mail: mkomareji@gmail.com*)*

ROLAND BOUFFANAIS
Singapore University of Technology and Design, 8 Somapah Road, 487372, Singapore
(e-mail: bouffanais@sutd.edu.sg*)*

Abstract

Distributed information transfer is of paramount importance to the effectiveness of dynamic collective behaviors, especially when a swarm is confronted with complex environmental circumstances. Recently, the signaling network of interaction underlying such effective information transfers has been revealed in the particular case of bird flocks governed by a topological interaction. Such biological systems are known to be evolutionary optimized, but are also constrained by the very nature of the signaling mechanisms—owing to intrinsic limitations in sensory modalities—enabling communication among individuals. Here, we propose that artificial swarm design can be tackled from the angle of signaling network design. To this aim, we use different network models to investigate the impact of some network structural properties on the effectiveness of a specific emergent swarming behavior, namely global consensus. Two new network models are introduced, which together with the well-known Watts–Strogatz model form the basis for an analysis of the relationship between clustering, shortest path and speed to consensus. A network-theoretic approach combined with spectral graph theory tools are used to propose some signaling network design principles. Eventually, one key design principle—a concomitant reduction in clustering and connecting path—is successfully tested on simulations of swarms of self-propelled particles.

Keywords: *interaction network, swarming systems, temporal networks*

1 Introduction

The sight of large numbers of animals moving together in unison has been an inexhaustible source of inspiration and inquiry for generations. In the last two decades, a large body of research has focused on gaining insight into some of the key

* Present address: Technical University of Denmark, Department of Electrical Engineering, Elektrovej, Building 326, 2800 Kgs. Lyngby, Denmark
† Present address: SRBIAU, Hesarak, Daneshgah Blvd, Tehran, Iran

elements underlying collective animal motion: e.g. decision making, synchronization, structures, and regulation (Sumpter, 2010). The connection with complex systems science is now apparent and with that comes a better understanding of self-organizing emergent behaviors such as birds flocking, fish schooling, locusts marching, amoebae aggregating, and humans crowding (Camazine *et al*., 2001; Vicsek & Zafeiris, 2012; Bouffanais & Yue, 2010; Moussaïd *et al*., 2011). Furthermore, some recent field and laboratory experiments have provided scientists with large-scale and high-resolution data sets (Ballerini *et al*., 2008; Katz *et al*., 2011; Butail & Paley, 2012). The post-processing and analysis of these highly resolved kinematic samples allow for a better understanding of the local interactions among individual agents within bird flocks or fish schools—what Sumpter calls the behavioral algorithm (Sumpter, 2006). According to Sumpter, the key to understanding collective behaviors lies in identifying this behavioral algorithm as well as how information flows between swarming agents (Sumpter, 2006).

Very recently, a growing body of work turned to the study of this problem of information transfer within a dynamic collective (Strandburg-Peshkin *et al*., 2013; Sumpter *et al*., 2008; Lemasson *et al*., 2013; Couzin *et al*., 2005). From the engineering standpoint, such effective information transfers highlight the existence of an underlying communication channel that takes the form of an interaction or signaling network (Komareji & Bouffanais, 2013b; Strandburg-Peshkin *et al*., 2013; Young *et al*., 2013). Animal collectives use this signaling network to effectively respond to changes in the surroundings: e.g. coordinated evasive maneuvers upon detection of a predator or collision avoidance. Such a network-theoretic approach has already been successfully considered to decipher some intricate social animal behaviors (Croft *et al*., 2008). However, the structure and dynamics of those social networks are vastly different from the structure and dynamics of signaling networks underpinning swarming behaviors. Indeed, swarm signaling networks (SSNs) are temporal and adaptive networks (Holme & Saramäki, 2012; Gross & Blasius, 2008) with a dynamics deeply interwoven with the agents' motion dynamics in the physical space. For instance, in the particular case of bird flocks governed by a topological interaction (Ballerini *et al*., 2008), the SSN has been found to be a small-world, homogeneous clustered network whose connectedness is key to yielding resilient swarming behaviors (Komareji & Bouffanais, 2013b). The knowledge of and access to the structural properties of the SSN revealed the high dynamic controllability of swarms (Komareji & Bouffanais, 2013b,a)—where few agents are capable of driving the dynamics of the swarm as a whole—as well as very effective consensus reaching processes (Shang & Bouffanais, 2014b).

Beyond the mechanistic and functional understanding of such evolutionary-optimized collective behaviors, many research groups are now turning to the design of artificial swarming systems (Hsieh *et al*., 2008; Naruse, 2013). The ultimate goal when designing such systems is to mimic some fundamental principles of collective animal behaviors with the objective to autonomously perform specific tasks. Such artificial swarms readily offer tremendous opportunities since they are freed from a large number of "constraints" inherent to biological systems: e.g. short-range signaling mechanisms, obstructed line of sight (Shang & Bouffanais, 2014a). It appears therefore that one of the keys to achieving successful artificial swarm designs lies with an effective design of the SSN. However, in practice, this is easier said than

https://doi.org/10.1017/nws.2016.5 Published online by Cambridge University Press

done given the lack of sound design principles in the form of relationship between parameters measuring the effectiveness of some specific swarming behaviors and canonical structural properties of networks for the SSN: e.g. clustering coefficient (CC), shortest connecting path (SP), degree distribution, centrality, connectedness, algebraic connectivity, etc. (Barrat *et al*., 2008).

Here, we provide the framework for analyzing such design principles for one of the most prevalent collective decision-making processes consisting in achieving global consensus—consensus means the convergence to a common state asymptotically or in a finite time among all group members through local interactions (Olfati-Saber *et al*., 2007). To the best of our knowledge, no clear relationship between the structural properties of the SSN and speed to consensus has ever been presented. Moreover, in their review paper, Arenas *et al*. (2008) mentioned the significant discrepancies in results for different network models when considering the related problem of synchronization in complex networks. According to Arenas *et al*. (2008), these discrepancies originate from studies where multiple non-independent parameters characterizing the network were concomitantly changed. This stresses the difficulty in carrying out thorough parametric studies on such networked systems. Indeed, in general, all canonical structural properties of a network bear a certain level of interdependence. For instance, Xu & Liu (2008) uncovered a clear relationship between spread of information in social networks and the CC.

In this paper, we establish how a group of agents can perform more effective emergent swarming behaviors through the specific design of the underlying SSN, which embodies how information flows through a swarm. By studying the SSN and its properties, the dynamics of a group of locally interacting agents can be analyzed from a radically different viewpoint as compared to classical observations in the physical space (Komareji & Bouffanais, 2013b; Vicsek & Zafeiris, 2012; Shang & Bouffanais, 2014a,b). Given the wide range of structural properties characterizing any network (CC, SP, degree distribution, directed/undirected character, etc.), establishing some general design principles is tremendously challenging if not unrealistic. However, when reducing the dimensionality of the design space to one or two, some design principles can be established and used for the design of more effective swarming rules. To this aim, three families of networks are considered in our study, as they allow us to tune the CC and SP for both directed and undirected networks having constraints similar as those encountered in real SSNs, in terms of average degree. First, we introduce these three one-parameter families of networks and study the influence of their respective control parameter on CC, SP, and the degree distribution. As a second step, we investigate the impact of CC and SP on the dynamics of the global consensus reaching process through a measure of the speed to consensus. The insights gained from the previous analysis are used in the final step to assess their effectiveness with simulations of swarms of self-propelled particles subjected to different neighborhood interaction rules.

2 Models of signaling networks

The network paradigm is used to represent the complex set of interactions among agents within a swarm. From a practical standpoint, the SSN is obtained through a bottom-up assembly of local interagent edges dependent on the neighborhood of

https://doi.org/10.1017/nws.2016.5 Published online by Cambridge University Press

interaction rule imposed on these agents. There are two canonical interaction rules: the first one based on a metric interaction distance and the other one based on a topological interaction distance (see Appendix 4 and Vicsek & Zafeiris, 2012). The metric neighborhood rule imposes that all agents within a certain fixed distance of each other, are neighbors, whereas a topological neighborhood rule specifies the fixed number of neighbors regardless of the distance separating them. For instance, the k-nearest neighbor rule is a paradigmatic example of topological neighborhood rules. Note that the metric neighborhood rule yields undirected SSNs, while SSNs designed using a k-nearest neighborhood are directed (Komareji & Bouffanais, 2013b) owing to the induced asymmetry in the relationship between agents—if agent j is in the neighborhood of agent i, then i needs not be in the neighborhood of j. Further details about the metric and topological interaction distances can be found in Appendix 4.

In this section, we introduce three families of complex networks generated through three distinct one-parameter algorithms for which we have an extensive indirect control over the value of the CC and SP. The first two families yield complex undirected networks while the third one is designed to generate complex directed networks. The first model is the well-known Watts & Strogatz (WS) model where it is possible to manipulate CC and SP by changing the control parameter p, the probability of rewiring randomly each edge—making the network go from a totally ordered network to a random one (Watts & Strogatz, 1998). The second model is based on an algorithm introduced by Holmes & Kim (HK) to grow a scale-free network with a tunable CC (Holme & Kim, 2002). The model is modified to ensure that the ratio between the number of nodes and edges, i.e. degree, remains constant on average, when networks with the same number of nodes are generated. This modification of the original HK model is suggested by the properties of the SSN based on a topological neighborhood of interactions, as well as to avoid pitfalls described by Arenas *et al.* in their review paper Arenas *et al.* (2008), in relation with parametric studies on complex networks. It is worth adding that the WS model intrinsically has a constant agent (i.e. vertex or node) to edge (i.e. link) ratio—in other words, it has a constant average degree—just like our modified Holme & Kim (MHK) model. Hence, these two undirected one-parameter models can be considered as rewiring algorithms of an original model under constraint—this constraint being the constant average degree. By construction, both the WS and MHK models produce undirected networks similarly to metric-based SSNs. As already mentioned, using a topological neighborhood of interaction rule such as the k-nearest neighbor rule, however, yields directed networks. Thus, a third one-parameter model is introduced. Based upon the topological neighborhood rule, this third model is designed to fix both the average in-degree and the out-degree regardless of the value of the control parameter. Using this so-called modified topological neighborhood of interaction (MTNI) model, it is found possible to establish a reciprocal mapping between the out-CC and the control parameter.

These three one-parameter models are described and analyzed in detail in Appendix . They are then used to investigate how different network properties—primarily CC and SP—affect the effectiveness of the consensus reaching process for the swarm. As a first step, we thoroughly analyze the relationship between control

https://doi.org/10.1017/nws.2016.5 Published online by Cambridge University Press

parameter and CC, SP, as well as the degree distributions of all the SSNs generated by the WS, MHK, and MTNI network models.

3 Results and Discussion

The speed of convergence to consensus is classically assessed by means of the spectral properties of graph Laplacians. The second smallest eigenvalue of the graph Laplacians λ_2—a.k.a. algebraic connectivity—quantifies that speed of convergence in the presence of a static network. This eigenvalue is greater than 0 if and only if the network is connected. This is a corollary to the fact that the number of times 0 appears as an eigenvalue in the graph Laplacian is the number of connected components in the network. Specifically, the magnitude of λ_2 reflects how well connected the overall network is, and has been used in analyzing the robustness and synchronizability of networks (Arenas *et al.*, 2008). Note that real SSNs are not static networks but instead are temporal networks. Therefore, it implies that the algebraic connectivity λ_2 is time dependent; this generalization is presented and discussed at great length in Shang & Bouffanais (2014b).

With the MHK, WS, and MTNI models introduced in Section 2 and detailed in Appendix , we are now able to directly measure and quantify the speed to consensus for families of SSNs corresponding to both undirected and directed information exchanges with variable CC, SP, as well as other network properties. This analysis of static networks is supplemented with numerical simulations of dynamic swarm behaviors where the network is changed at each iteration step. The numerical results obtained are ultimately compared with the spectral predictions based on the algebraic connectivity.

3.1 Spectral analysis of the SSNs

For the spectral analysis of undirected networks the normalized graph Laplacian (Chung, 1996), defined as

$$\widetilde{\mathbf{L}} = \mathbf{D}^{-\frac{1}{2}}(\mathbf{D} - \mathbf{A})\mathbf{D}^{-\frac{1}{2}}, \tag{1}$$

is used, with $\mathbf{A}$ and $\mathbf{D}$ being the adjacency matrix and the degree matrix, respectively. Using $\widetilde{\mathbf{L}}$ has the advantage of being similar to using the time-dependent graph Laplacian matrix describing a swarm whose agents have metric local interactions. This is aligned with the goal of the current paper, i.e. finding ways to improve the speed of reaching consensus by manipulating classical SSNs.

In Appendix , we have shown how the WS and MHK models allow us to generate networks with varying CC and SP through the tuning of control parameters. The procedure is here applied again but now to obtain the second smallest eigenvalue λ_2 of $\widetilde{\mathbf{L}}$. By doing so, we are able to plot the variations of λ_2 as a function of CC and SP. Note that for all three models, the CC is bounded within the intervals found earlier. The variations of λ_2 in terms of CC and SP are obviously represented by a line of points corresponding to given values of the control parameters p and P. These variations are shown in Figure 1 for both undirected models.

First, we note that when varying the control parameters, the changes in CC and SP are quite different for the WS and MHK models. Very little variation of the

https://doi.org/10.1017/nws.2016.5 Published online by Cambridge University Press

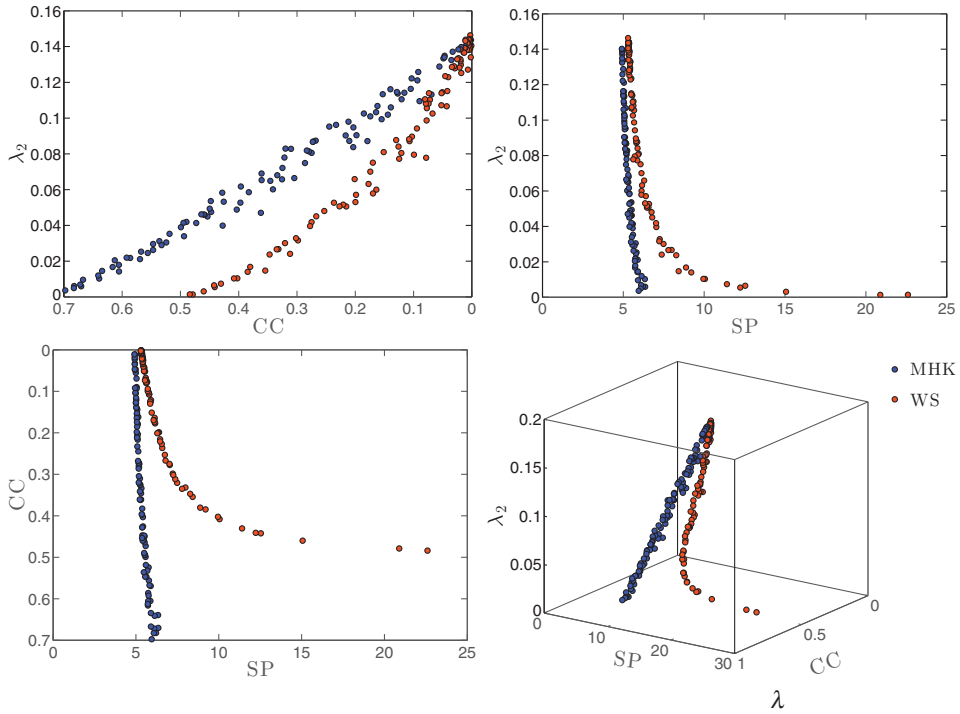

Fig. 1. Speed of reaching consensus measured using the most significant pole (λ_2). Each data point represents a network designed either using the WS model (red) or the MHK model (blue). All networks considered possess $N = 1,000$ nodes and an average degree of 4 (resp. 3.992) for the WS (resp. MHK) model. (Color online)

SP is observed with the MHK model for CC varying between 0 and approximately 0.7. As is well-known, the WS model yields significant variations of the SP with the CC (Watts & Strogatz, 1998). Furthermore, it is observed in Figure 1 that λ_2 tends towards the same value for networks designed with the two different models when the respective CC and SP converge towards the same values, even though we have found the degree distributions to be quite different for both the WS and MHK models. This result is noteworthy as it seems to contradict the frequently encountered statement that the degree distribution is key to many global outcomes of dynamic networked systems. However, it is difficult to conclude that for sure as the range of values for k is rather small in all SSNs owing to the small size of the network and the limited number of interagent connections. It is worth recalling here that the values found for λ_2 depend on the number of agents, i.e. the number of nodes N of the SSNs. All calculations were performed with $N = 1,000$ agents in order to minimize the number of parameters in our study.

Using the WS model, it can be shown that λ_2 does not necessarily increase when the SP is decreased as can be seen in Figure 2. However, there seems to be a clear relationship between the SP and λ_2 when CC is kept constant. That observation suggests that λ_2 can be predicted if CC, SP, and number of agents are known. Reducing CC while keeping SP constant or non-increasing is thus found to increase the speed to consensus.

https://doi.org/10.1017/nws.2016.5 Published online by Cambridge University Press

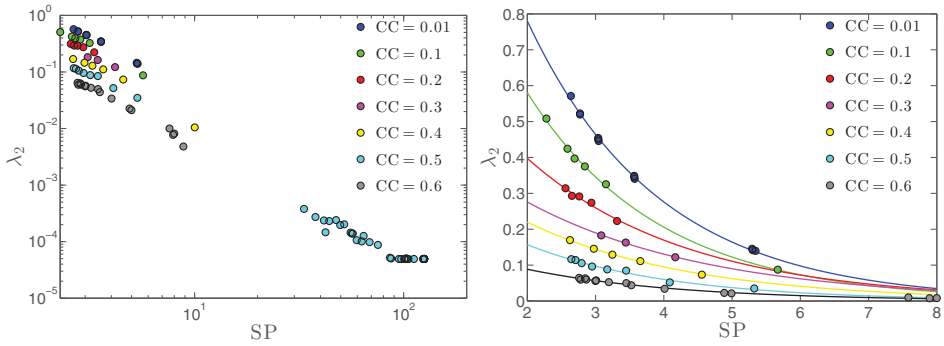

Fig. 2. Variations of the algebraic connectivity with the shortest connecting path for different values of the clustering coefficient for small-world networks generated from the WS model. Each data point represents a network consisting of $N = 1,000$ nodes. The average degree varies between 4 and 36 leading to a non-constant average degree. Left: log-log scale. Right: linear scale with the colored lines being exponential fits corresponding to a specific CC with an error margin of $\pm 2\%$. (Color online)

Before testing if a similar relationship with directed networks exists, we need to define the concept of Laplacian matrix for directed networks. The Laplacian matrix has to be redefined because the in- and out-degree of a node need not be the same in the case of a directed network, thus preventing us from using the previously introduced normalized Laplacian graph. Thus, we use the following definition for the Laplacian matrix:

$$\mathbf{L} = \mathbf{D}_{\text{out}}^{-1}(\mathbf{D}_{\text{out}} - \mathbf{A}_{\text{out}}), \tag{2}$$

where $\mathbf{A}_{\text{out}}$ and $\mathbf{D}_{\text{out}}$ are the out-adjacency matrix and the out-degree matrix, respectively. This is indeed an appropriate choice as neighbors are pointed at with outward edges in the directed SSN. Note that in the particular case of SSNs, we assume the networks to be strongly connected otherwise, we would have to deal with several swarms instead of just one. Consequently, the graph Laplacian defined by Equation (2) will lead to consensus since the union of the dynamically evolving SSNs have a spanning tree frequently enough.

Following the method used for undirected networks, a plot of the variations of the real part of λ_2, SP and CC_{out} is shown in Figure 3. An out-degree of 10 is chosen so that the generated networks are strongly connected with $N = 1,000$ nodes (Komareji & Bouffanais, 2013b). We recover a trend similar to the one observed previously with undirected networks; namely the speed to consensus as measured by $\text{Re}(\lambda_2)$ monotonously increases with a decreasing CC_{out} for non-increasing SP. This trend emphasizes the following very important design principle that it is not only important to reduce the SP of a network—as is done in many studies such as Olfati-Saber (2005) for instance—but the CC also needs to be reduced, in order to speed up the global consensus reaching process, while accounting for the drastic constraints imposed by the interaction rule to the degree distribution. Note that this statement is consistent with the result by Xu & Liu (2008) showing a clear relationship between spread of information in social networks and the CC.

https://doi.org/10.1017/nws.2016.5 Published online by Cambridge University Press

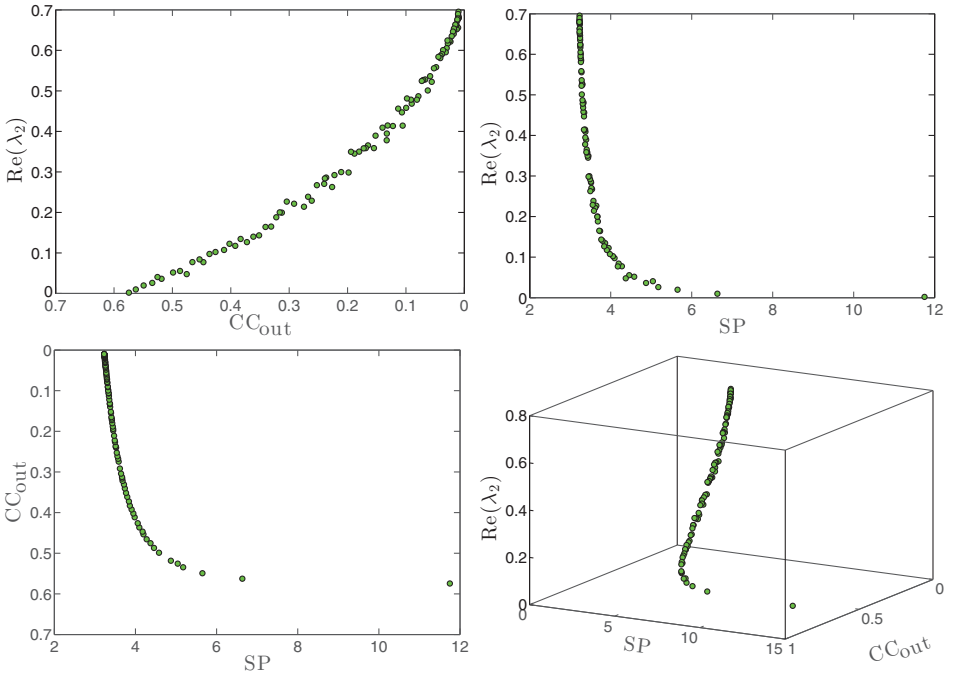

Fig. 3. Speed of reaching consensus measured using $\mathrm{Re}(\lambda_2)$. Each data point represents a network designed using the MTNI model, with $\mathscr{P}$ varying between 0 and 1. All networks considered possess $N = 1,000$ nodes and a fixed out-degree of 10. The case $\mathscr{P} = 0$, associated with the pure TNI model corresponds to the rightmost point with the highest clustering coefficient. (Color online)

3.2 Simulations of artificial swarming behaviors

The insights gained in Section 3.1 enable us to turn to actual simulations of swarm dynamics with specifically designed signaling networks. As previously discussed, depending on the neighborhood interaction rule, these SSNs can either be directed or undirected. For the two canonical neighborhood schemes, namely the metric and topological neighborhood of interaction, it was found numerically that the CC is approximately 0.6 with 2D swarming models (Komareji & Bouffanais, 2013b), and also analytically in the metric interaction case (Dall & Christensen, 2002). Hence, speeding up the consensus reaching process could be achieved by modifying the topological structure of the SSN following the design principle devised in Section 3.1. Specifically, a reduction in the CC without any increase in the SP was found to yield a significantly higher real part of λ_2. Of course, such a strategy can only be applied to artificial swarms where the neighborhood interaction rule can be designed and imposed unlike natural systems. Therefore, this effort could potentially lead to tremendous operational improvements in the functioning of robotic swarms as well as mobile sensory networks.

Before focusing on simulations of swarms, it is worth noting an important difference between swarms of inanimate agents and swarms of living units. This difference resides in the ability of the latter to collectively process and respond to information in the form of signals and stimuli. There is no doubt that it contributes

https://doi.org/10.1017/nws.2016.5 Published online by Cambridge University Press

to the greater complexity and variety of collective behaviors observed in the natural world—i.e. for swarms of living organisms—as compared to those encountered in the physical world—i.e. for swarms of inanimate agents. The term "swarm intelligence" is colloquially used to refer to such emergent and adaptive collective responses of groups of simple agents. The past two decades have experienced substantial work aimed at mimicking specific collective behaviors, where each individual agent follows a very simple set of local rules, without having access to any knowledge about the overall swarm and pattern in motion. These collective behaviors are quite resilient and show a great level of adaptivity. Robustness and flexibility are very appealing features for an engineering system.

Following the work by Komareji & Bouffanais (2013b), we consider a collective of N identical interacting agents moving at the same speed denoted as v_0 (Vicsek & Zafeiris, 2012). Each individual agent i, at any given instant t, is assumed to be fully characterized by a given state variable $\psi_i(t)$. Such a generic state variable may represent widely different characteristics depending on the nature of the group considered: e.g. kinematic variables for fish in a school, birds in a flock or robots in an artificial swarm, space available for a pedestrian on a congested sidewalk, etc. Here, the state variable simply reduces to the direction of travel and the achievement of swarm consensus therefore yields an alignment of all the agents, in other words a polarized swarm. Hence, from a formal standpoint, by reaching a consensus, we mean asymptotically converging to a one-dimensional agreement in space characterized by $\psi_1 = \psi_2 = \cdots = \psi_N$ (Olfati-Saber *et al.*, 2007).

In the dynamical model considered, the adaptive and interacting swarming agents are modeled as self-propelled particles for which the biological details of the internal origin of an agent's thrust is considered to be irrelevant. Such SPP-based models are a good representation of collective animal behaviors (Vicsek & Zafeiris, 2012). Here, these SPPs are moving about a two-dimensional plane with constant speed v_0 and subject to a mix of a local interactions and random ones. As mentioned previously, each agent i is fully characterized by its direction of travel—in other words, here $\psi_i(t) = \theta_i(t)$—related to the agent's velocity through $\mathbf{v}_i = v_0 \cos\theta_i \hat{x} + v_0 \sin\theta_i \hat{y}$. The local synchronization protocol, based on relative states, is strictly equivalent to a local linear alignment rule which mathematically can be stated as

$$\theta_i(t + \Delta t) = \theta_i(t) + \frac{\Delta t}{k_i} \sum_{j=1}^{k_i} (\theta_j(t) - \theta_i(t)), \tag{3}$$

where k_i is the out-degree of node i. For all simulations, the following values were taken: $v_0 = 0.03$ and $\Delta t = 1$ (Vicsek *et al.*, 1995; Komareji & Bouffanais, 2013b). The agents were able to move in a square domain of dimension $\ell = 10$ having periodic boundaries. As is well-known with such standard SPP models, the values of v_0 and Δt have practically no effect on the swarm dynamics, while the swarm density $\rho = N/\ell^2$ has to be kept sufficiently high so as to maintain a global ordering of the swarm (Vicsek & Zafeiris, 2012).

As stressed in Shang & Bouffanais (2014b), the dynamics of this directed SSN is intricately connected to the dynamics of the agents since they are embedded in the physical space. Signaling network structure/topology and information transfer dynamics change on the same time scale and are strongly interwoven. Throughout

https://doi.org/10.1017/nws.2016.5 Published online by Cambridge University Press

the complete dynamical process, the signaling network maintains a constant number of nodes and some edges are broken while new ones are being created following the interaction rule. The rate at which network edges are changing is governed by the pace of the physical dynamics of the swarm. Hence, we consider here the general case of switching networks of interaction. Such switching events intrinsically occur at non-uniform time intervals. As detailed in Shang & Bouffanais (2014b), one can assume without loss of generality that those switching events are evenly distributed in time with the time interval between switching events corresponding to the decorrelation time scale τ of the matrix of correlations $C_{ij} = \langle \mathbf{s}_i \cdot \mathbf{s}_j \rangle$ for the normalized velocity $\mathbf{s}_i = \mathbf{v}_i / v_0$. As all agents move at constant speed v_0, the decorrelation time scale is therefore strictly equivalent to the spatial decorrelation time scale, which given our hybrid interaction rule is directly related to the value of k.

The consensus level within the swarm is measured by the following order parameter:

$$\varphi = \frac{1}{N} \sum_{j=1}^{N} \frac{v_j(t)}{v_0} = \frac{1}{N} \sum_{j=1}^{N} \exp\left(\mathrm{i}\theta_j(t)\right), \tag{4}$$

with v_j the velocity of agent j in complex notation. In the particular case of self-propelled particles, the order parameter φ represents the alignment of the collective. The simulations were carried out with $N = 1,000$ agents, for five different values of the number, r, of randomly rewired SSN edges. The consensus within the swarm in the physical space is measured by means of the order parameter φ and simultaneously, we keep track of the variations of CC, SP, and the algebraic connectivity. It is important keeping in mind that the SSN has a dynamics that is evolving hand in hand with the dynamics of the mobile agents in the physical space. In other words, signaling network structure and information dynamics change on the same time scale and are strongly interwoven. In practice, the average values of φ, CC ($\mathrm{CC_{out}}$ in the directed cases), SP, and λ_2 ($\mathrm{Re}(\lambda_2)$ in the directed cases) were considered using a statistically ample enough sampling of 50 distinct swarm dynamics all initiated with agents randomly distributed in space and also having random velocity directions.

First, we consider the case for which a directed flow of information governs the swarm dynamics. Specifically, all swarming agents interact with exactly $k = 10$ other agents, i.e. the out-degree of the associated SSN is uniformly 10. Out of the $k = 10$ influencing neighbors, a certain number r of them are taken at random, while the $t = k - r$ others are chosen following the t-nearest neighbor rule in the topological sense (see Appendix 4). By varying r between 0—purely topological—and k—purely random, one is able to generate different SSNs leading to different swarming behaviors. Practically, this is equivalent to the MTNI model introduced previously. The results are shown in Figure 4 for five values of r with both global random rewiring—creating a new edge with any agent within the swarm picked at random (solid lines)—and local random rewiring—creating a new edge with any agent picked at random within a disk of radius 2 (dashed lines). Note that the speed to consensus measured directly by means of the variations of φ with time in the physical space, for different values of r, are in total agreement with the SSN network-theoretic measure of speed through $\mathrm{Re}(\lambda_2)$, and that for both the global

https://doi.org/10.1017/nws.2016.5 Published online by Cambridge University Press

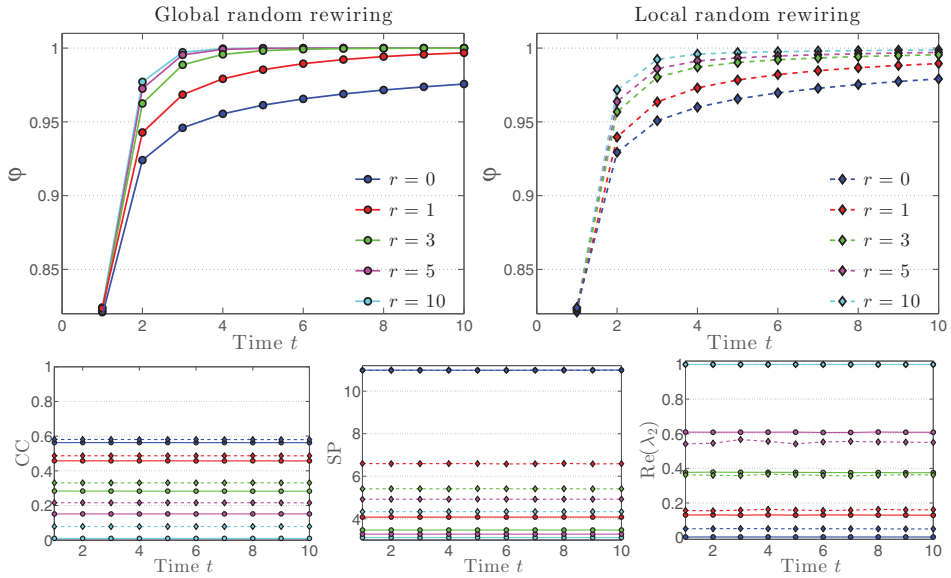

Fig. 4. Dynamics of a swarm comprising $N = 1,000$ agents moving about a square domain of dimension ℓ, corresponding to an agent density $\rho = N/\ell^2 = 10$. Each individual interacts with $k = \tau + r = 10$ other swarming agents according to the update rule (3): τ agents being nearest neighbors and r are chosen at random. At each iteration step, the alignment of the swarm in the physical space is measured through the order parameter φ, and the SSN is formally constructed thus enabling the computation of $\mathrm{CC}_{\mathrm{out}}$, SP and $\mathrm{Re}(\lambda_2)$. The values for $\mathrm{Re}(\lambda_2)$ are normalized using the maximum values obtained in the case $r = 10$, independently for the global and local random rewiring. Each color represents a specific number r of SSN edges randomly wired for each agent. The solid lines correspond to the case of a global random rewiring; that is a new edge is randomly created with an agent anywhere within the swarm, irrespective of the distance separating them. The dashed lines correspond to the case of a local random rewiring; that is a new edge is randomly created with an agent located within a disk of radius 2. (Color online)

and local random rewiring. It is worth noticing that except for the order parameter φ, all other quantities are practically constant on average as the swarm evolves towards consensus, and that for all values of r considered. As is well known, adding random links—that is increasing r—does speed up the consensus reaching process. This fact can obviously be understood from the SP standpoint. The random rewiring of edges drastically reduces the SP, thereby shortening the information travel path, hence improving the information reaching process globally. Nonetheless, one should not lose track of the important fact that in this particular case, the reduction in SP is simultaneously accompanied by a reduction of the CC. These last points are in complete agreement with the SSN design principle devised in Section 3.1, and further highlight the importance of tracking the interdependence of several network properties, such as CC and SP in the present case. Finally, and as expected, the global random rewiring of the SSN is more effective than the local one. Indeed, the global random rewiring scheme yields a higher reduction in both CC and SP as compared to its local counterpart. This provides further evidence in support of our SSN design principle.

https://doi.org/10.1017/nws.2016.5 Published online by Cambridge University Press

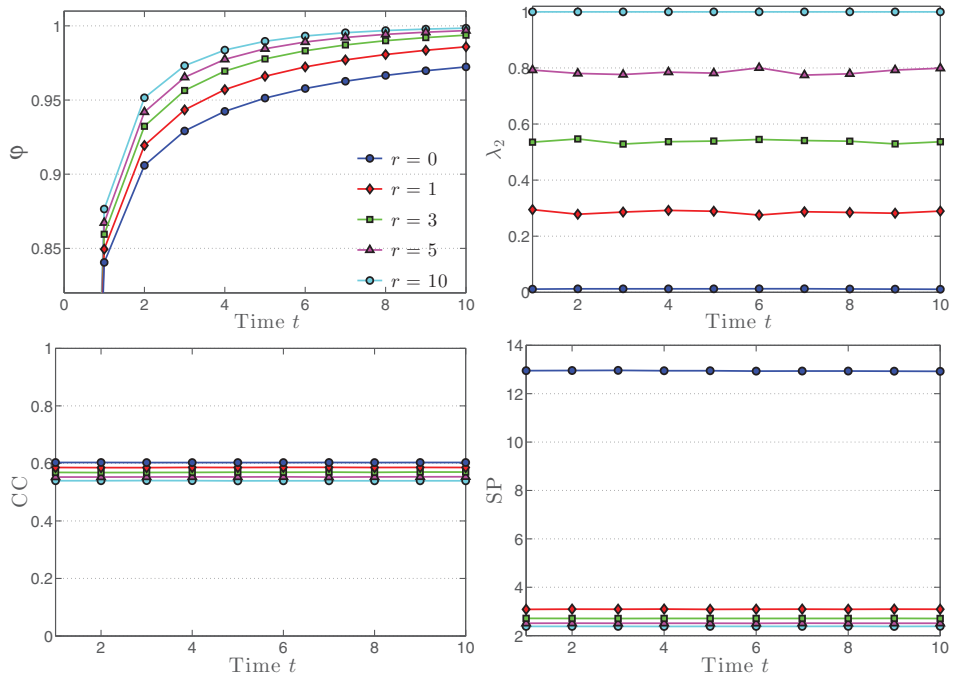

Fig. 5. Dynamics of a swarm comprising $N = 1,000$ agents moving about a square domain of dimension ℓ, corresponding to an agent density of $\rho = N/\ell^2 = 10$. Each individual interacts with all neighbors located in a disk of radius $R_0 = 1/\pi$ (metric interaction rule) to impose an average degree of 10, except for r edges randomly rewired with agents chosen anywhere within the swarm (global random rewiring). The update rule (3) is used with $k_i - r$ neighbors in the disk of radius $R_0 = 1/\pi$ and r other neighbors chosen at random irrespective of the distance separating them. At each iteration step, the alignment of the swarm in the physical space is measured through the order parameter φ, and the SSN is formally constructed thus enabling the computation of CC, SP, and λ_2. The values for λ_2 are normalized using the maximum values obtained in the case $r = 10$. Each color represents a specific number r of SSN edges randomly wired for each agent. (Color online)

As a last step, we envisage swarm dynamics governed by an undirected flow of information. Such a dynamics is achieved when the underlying SSN is an undirected network. To that aim, we consider an undirected global random rewiring of SSNs based on a metric interaction distance. Specifically, a swarm of $N = 1,000$ agents interacting with all agents located in a disk of radius $R_0 = 1/\pi$ is simulated. The value of R_0 is chosen such that the resulting average degree $\langle k \rangle$ is very close to 10—fixed value of the out-degree used in the previous directed case. Swarming agents having more than r other agents in their metric neighborhood are subjected to a global random rewiring of r edges of their SSN, operated in a similar fashion to the directed case. The results for this metric-based swarm dynamics in both the physical space (φ) and network space (CC, SP, and λ_2) are presented in Figure 5. Interestingly, the conclusions gathered in the directed case still apply in the present undirected case. The only notable difference pertains to the effects of the number r of edges rewired at random. Indeed, a much larger number of edges need to be rewired to achieve significant improvements in terms of dynamics of the alignment, i.e. to accelerate the increase in swarm alignment φ. This observation in the physical

https://doi.org/10.1017/nws.2016.5 Published online by Cambridge University Press

space is corroborated by the fact that in the metric case, the increase in r leads to very minimal decrease in CC. This point highlights one more time the importance of reducing the CC to gain a significant speed up in the polarization of the swarm. Furthermore, it is very interesting to note that the sharp drop in SP with even just one edge randomly rewired fails to yield significant increase in speed to consensus. This last point suggests that a reduction in CC is more beneficial than a reduction in SP for the speeding up of self-organizing emergent behaviors.

It is worth noticing that λ_2, SP, and CC for the undirected case, or CC_{out} for the directed case are constant over time. Such behavior is not surprising, since there is almost no transient dynamics in the self-organization of the SSNs. The topology and properties of the SSNs are instantly imposed by the particular interaction distance in the physical space (Dall & Christensen, 2002; Komareji & Bouffanais, 2013b).

4 Conclusions

Social transmission of information is critical to the effectiveness of emergent swarming behaviors. With the signaling network of interaction accessible, the effectiveness of swarm dynamics can directly be apprehended and improved from the angle of signaling network design.

In this paper, we report a first attempt in designing signaling network for artificial swarms with the aim of bettering the emergence of order through one specific example: the acceleration of the consensus reaching process. We believe that the approach undertaken in our study is general enough to be extended to other possible scenarios and other types of self-organizing behaviors. To the best of our knowledge, no general design principles for signaling networks are available. On the contrary, design principles for networks tend to be lacking in view of some contradicting conclusions reported in the literature (Arenas *et al.*, 2008). Here, the thorough study of three distinct network models—two undirected (WS and MHK) and one directed (MTNI)—allowed us to establish clear relationships between CC, SP, and speed to consensus. All three network models use a unique control parameter—different for each model—enabling us to investigate a large interval of values for the CC and SP. These models highlighted the known interdependency between CC and SP, but here in a particular framework, since SSNs are intrinsically constrained to have a fixed average degree.

It is important to study both directed and undirected networks because depending on the swarm design and the choice of neighborhood of interaction, the transmission of behavioral information may either be unidirectional or bidirectional. As was discussed, a metric interaction distance leads to bidirectional information exchanges associated with an undirected network. On the contrary, a topological interaction in the physical space yields unidirectional transmission of information represented with a directed network. With these three network families at hand, we were able to perform a parametric spectral graph analysis in both the directed and undirected cases, leading to a quantitative metrics of the speed to consensus. We established the variations of the algebraic connectivity (or its real part in the directed case) with both CC and SP, with different degree distributions but at fixed average degree. This analysis led to the establishment of the following design principle for both directed and undirected SSNs: it is not only important to reduce the SP—as is classically

https://doi.org/10.1017/nws.2016.5 Published online by Cambridge University Press

recommended in many studies—but the CC also needs to be reduced—action which is often overlooked. This design principle, and in particular the part pertaining to the CC, is consistent with some studies dealing with social networks—networks that are structurally and temporally quite different from SSNs—e.g. relation between social information transmission and CC in social networks (Xu & Liu, 2008).

As a final step, the established design principle was implemented and tested in simulations of swarm dynamics of autonomous interacting self-propelled agents. Specific agent interaction rules were devised to produce SSNs with the desired properties in terms of SP, but more importantly in terms of CC. The interaction rules were tinkered with by performing a certain number of random rewiring of topological and metric interagent interaction sets at the global swarm level. That is, short-distance interactions usually confined at the neighborhood level were randomly replaced by possibly long-distance interactions across the entire swarm. A more local random rewiring was further tested in the directed topological case. with that, both directed and undirected SSN designs were tested. For all simulated cases, a reduction in CC along with a decrease in the SP led to an acceleration of the convergence of the swarm to global consensus. Such results provide further confirmation of the validity of our design principle for SSN and also suggest the lack of relevance of the degree distribution in the SSN design process. Finally, in the particular case of a metric interaction distance, the global random rewiring yields a drastic reduction in SP but with a very limited decrease in CC. In the physical space, the polarization of the swarm is not accelerated as much as in the topological case. This final observation suggests that a reduction in CC is more advantageous than a reduction in SP for the speeding up of self-organizing emergent behaviors.

Conflict of interests

The authors declare having no conflict interests of any kind, financial or intellectual.

Acknowledgments

We thank Dr. Yilun Shang for fruitful and stimulating conversations. This work was supported by a SUTD–MIT International Design Centre (IDC) Grant (A.S. & M.K.) and by a grant from the Temasek Lab (TL@SUTD) under the STARS project (R.B.).

References

Arenas, A., Díaz-Guilera, A., Kurths, J., Moreno, Y., & Zhou, C. (2008). Synchronization in complex networks. *Physics Reports,* **469**, 93–153.

Ballerini, M., Cabibbo, N., Candelier, R., Cavagna, A., Cisbani, E., Giardina, I., . . . Zdravkovic, V. (2008). Interaction ruling animal collective behavior depends on topological rather than metric distance: Evidence from a field study. *Proceedings of the National Academy of Sciences USA,* **105**, 1232–1237.

Barrat, A., Barthélemy, M., & Vespignani, A. (2008). *Dynamical processes on complex networks.* Cambridge, U.K.: Cambridge University Press.

Bouffanais, R. (2016). *Design and control of swarm dynamics.* Heidelberg: Springer.

Bouffanais, R., Weymouth, G. D., & Yue, D. K. P. (2011). Hydrodynamic object recognition using pressure sensing. *Proceedings of the Royal Society A,* **467**, 19–38.

Bouffanais, R., & Yue, D. K. P. (2010). Hydrodynamics of cell-cell mechanical signaling in the initial stages of aggregation. *Physical Review E,* **81**, 041920.
Butail, S., & Paley, D. A. (2012). Three-dimensional reconstruction of the fast-start swimming kinematics of densely schooling fish. *Journal of The Royal Society Interface,* **9**, 77–88.
Camazine, S., Deneubourg, J.-L., Franks, N. R., Sneyd, J., Theraulaz, G., & Bonabeau, E. (2001). *Self-organization in biological systems*. Princeton, NJ: Princeton University Press.
Chung, F. R. K. (1996). *Spectral Graph Theory*. (CBMS Regional Conference Series in Mathematics, No. 92). Providence, RI: American Mathematical Society.
Coombs, S., & Montgomery, J. C. (1999). The enigmatic lateral line system. In R. R. Fay, & A. N. Popper (Eds.), *Comparative hearing: Fish and amphibians, springer handbook of auditory research* (pp. 319–362). New York, NY: Springer-Verlag.
Couzin, I. D., Krause, J., Franks, N. R., & Levin, S. A. (2005). Effective leadership and decision making in animal groups on the move. *Nature,* **433**, 513–516.
Croft, D. P., James, R., & Krause, J. (2008). *Exploring animal social networks*. Princeton, NJ: Princeton University Press.
Dall, J., & Christensen, M. (2002). Random geometric graphs. *Physical Review E,* **66**, 016121.
Fagiolo, G. (2007). Clustering in complex directed networks. *Physical Review E,* **76**, 026107.
Ginelli, F., & Chaté, H. (2010). Relevance of metric-free interactions in flocking phenomena. *Physical Review Letters,* **105**, 168103.
Gross, T., & Blasius, B. (2008). Adaptive coevolutionary networks: A review. *Journal of the Royal Society Interface,* **5**, 259–271.
Hemelrijk, C. K., & Hildenbrandt, H. (2012). Schools of fish and flocks of birds: Their shape and internal structure by self-organization. *Interface Focus,* **2**, 726–737.
Holme, P., & Kim, B. J. (2002). Growing scale-free networks with tunable clustering. *Physical Review E,* **65**, 026107.
Holme, P., & Saramäki, J. (2012). Temporal networks. *Physics Reports,* **519**, 97–125.
Hsieh, M. A., Kumar, V., & Chaimowicz, L. (2008). Decentralized controllers for shape generation with robotic swarms. *Robotica,* **26**(8), 691–701.
Katz, Y., Tunstrøm, K., Ioannou, C. C., Huepe, C., & Couzin, I. D. (2011). Inferring the structure and dynamics of interactions in schooling fish. *Proceedings of the National Academy of Sciences USA,* **108**, 18720–18725.
Komareji, M., & Bouffanais, R. (2013a). Controllability of a swarm of topologically interacting autonomous agents. *International Journal of Complex Systems in Science,* **3**, 11–19.
Komareji, M., & Bouffanais, R. (2013b). Resilience and controllability of dynamic collective behaviors. *PLoS one,* **8**, e82578.
Lemasson, B. H., Anderson, J. J., & Goodwin, R. A. (2013). Motion-guided attention promotes adaptive communications during social navigation. *Proceedings of the Royal Society B,* **280**, 20122003.
Liu, Y.-Y., Slotine, J.-J., & Barabási, A.-L. (2011). Controllability of complex networks. *Nature*, **473**, 167–173.
Liu, Y.-Y., Slotine, J.-J., & Barabási, A.-L. (2012). Control centrality and hierarchical structure in complex networks. *PLoS one,* **7**(9), e44459.
Moussaïd, M., Helbing, D., & Theraulaz, G. (2011). How simple rules determine pedestrian behavior and crowd disasters. *Proceedings of the National Academy of Sciences USA,* **108**, 6884–6888.
Naruse, K. (2013). Velocity correlation in swarm robots with directional neighborhood. In S. Lee, H. S. Cho, K. J. Yoon, & J. M. Lee (Eds.), *Intelligent autonomous systems 12* (pp. 843–851). Advances in Intelligent Systems and Computing. Berlin: Springer-Verlag.
Olfati-Saber, R. (2005). Ultrafast consensus in small-world networks. *Proc. Am. Control Conf.*, pp. 2371–2378.
Olfati-Saber, R. (2006). Flocking for multi-agent dynamic systems: Algorithms and theory. *IEEE Transactions on Automatic Control*, **51**, 401–420.
Olfati-Saber, R., Fax, J. A., & Murray, R. M. (2007). Consensus and cooperation in networked multi-agent systems. *Proceedings of the IEEE,* **95**(1), 215–233.
Shang, Y., & Bouffanais, R. (2014a). Consensus reaching in swarms ruled by a hybrid metric-topological distance. *European Physical Journal B,* **87**, 294.

Shang, Y., & Bouffanais, R. (2014b). Influence of the number of topologically interacting neighbors on swarm dynamics. *Scientific Reports,* **4**, 4184.

Strandburg-Peshkin, A., Twomey, C. R., Bode, N. W., Kao, A. B., Katz, Y., Ioannou, C. C., ref. . . Couzin, I. D. (2013). Visual sensory networks and effective information transfer in animal groups. *Current Biology,* **23**(17), R709–R711.

Sumpter, D., Buhl, J., Biro, D., & Couzin, I. (2008). Information transfer in moving animal groups. *Theory Bioscience,* **127**, 177–186.

Sumpter, D. J. T. (2006). The principles of collective animal behaviour. *Philosophical Transactions of the Royal Society B,* **361**, 5–22.

Sumpter, D. J. T. (2010). *Collective animal behavior*. Princeton, NJ: Princeton University Press.

Vicsek, T., Czirók, A., Ben-Jacob, E., Cohen, I., & Shochet, O. (1995). Novel type of phase-transition in a system of self-driven particles. *Physical Review Letters,* **75**, 1226–1229.

Vicsek, T., & Zafeiris, A. (2012). Collective motion. *Physics Reports,* **517**, 71–140.

Watts, D. J., & Strogatz, S. H. (1998). Collective dynamics of "small-world" networks. *Nature,* **393**, 440–442.

Xu, W., & Liu, Z. (2008). How community structure influences epidemic spread in social networks. *Physica A,* **387**, 623–630.

Young, G. F., Scardovi, L., Cavagna, A., Giardina, I., & Leonard, N. E. (2013). Starling flock networks manage uncertainty in consensus at low cost. *PLoS Computational Biology,* **9**(1), e1002894.

Appendix A: Interaction distances in swarming systems

The basic mechanistic functioning of collective motion is well understood as being the result of multiple uncoordinated local interactions between individuals. The central importance of these local interactions have led scientists to experiment with various local interaction rules, often with the aim to reproduce fine details of some specific swarming behaviors. Two broad classes of interaction rules can be discerned, each based on the definition of a specific interaction distance. The first group based on a metric distance, was the first considered and has attracted a tremendous amount of attention (see Bouffanais 2015 and references therein). In this metric interaction distance framework, each swarming agent exchanges information with all other agents located at a fixed and given distance—assumed to be the same for all (Hemelrijk & Hildenbrandt, 2012). The metric distance was only recently challenged following the analysis of empirical data for the dynamics of flocks of starlings (Ballerini *et al*., 2008) as well as results from the dynamics of human crowds (Ginelli & Chaté, 2010; Moussaïd *et al*., 2011). By reconstructing the three-dimensional positions of individual birds in airborne flocks of a few thousand members, Ballerini *et al*. showed that the interaction does not depend on the metric distance, as most current models and theories assume, but rather on the topological distance. They discovered that each bird interacts on average with a fixed number of neighbors (six to seven), rather than with all neighbors within a fixed metric distance.

Essentially, both distances are associated with distinct physiological (resp. technological) limitations of living (resp. artificial) agents. Specifically, the metric neighborhood of interaction finds its origin in the limited sensory range of individuals. Indeed, a fish in a school can only interact with other fish it can perceive either through vision or lateral line sensing (Coombs & Montgomery, 1999; Bouffanais *et al*., 2011). On the other hand, the topological neighborhood of interaction stems

https://doi.org/10.1017/nws.2016.5 Published online by Cambridge University Press

from the limited information-processing capabilities of individuals. All living or artificial agents possess limited cognitive and information-processing capabilities enabling them to socially interact with a fixed number of other agents. However, in real-life situations and depending on their positions within the swarm, individuals may found themselves limited either by their sensory apparatuses or by their internal information-processing system. Also, with a topological neighborhood, one has to be watchful for the possibility of the topological distance becoming too large so that the interaction or information exchange could not take place. In practice, that can potentially happen with very low density swarms or when some individual agents become widely separated from the swarm. The rule of k-nearest neighbors epitomizes the topological paradigm.

Finally, it is worth adding that a purely metric or purely topological distance is unable to account for this inhomogeneity in limiting factors within the group. This has led some researchers to propose a hybrid interaction distance that integrates both limitations in terms of sensory range as well as information processing (Shang & Bouffanais, 2014a).

Appendix B: Details about models of signaling networks

B.1 Undirected networks

To analyze the impact of the CC on speed to consensus for undirected networks, the MHK model is introduced and compared with the WS model. Both models provide a tunable CC by controlling one single parameter at constant average degree. Interestingly, both MHK and WS models yield different degree distributions thereby allowing us to further assess the influence of the degree distributions on the consensus reaching process. The MHK model is inspired by an algorithm proposed by Holme & Kim (2002) devised to design scale-free networks with a tunable CC. It can readily be described by the following simple steps:

1. Create four nodes;
2. Add edges so that each node is connected to exactly two other nodes;
3. Randomly link one of the existing nodes to a newly added one;
4. Given a probability P either: (i) add an edge between the new node and another node in the network that increases the number of triangles (in the CC sense), or (ii) add an edge that does not increase the number of triangles;
5. Repeat from step 3 until the desired number of nodes N is attained.

A graphical representation of the above successive steps is shown in Figure B1.

The one-to-one relationships between the control parameters—P for the MHK model and p for the WS model—and CC or SP are shown in Figure B2. Interestingly, for the MHK model, the variations of the CC are found to be practically linear with P, while the SP increases extremely moderately in comparison with the same results for the WS model. Specifically, for each value of the probability P, the average CC and SP and the associated standard deviations are calculated using a statistically ample enough sample of 50 networks generated from the MHK model with $N = 1,000$ nodes and $E = 3,992$ edges. The constant average degree is thus equal to the fixed degree $\langle k \rangle$. By construction, an increase in the value of the

https://doi.org/10.1017/nws.2016.5 Published online by Cambridge University Press

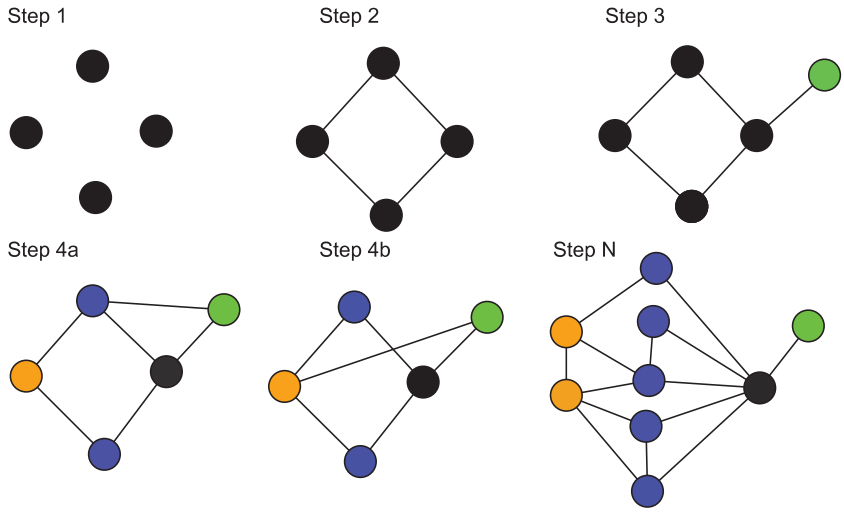

Fig. B1. Illustration of the successive steps in the MHK model. A black node represents an unchanged node at any given step, the green node is the newly added node at step 3. At step 1, four nodes are created. At step 2, the nodes are linked together so all nodes have exactly two neighbors. At step 3, the green node is added and attached at random to one of the four black nodes in the existing network. At step 4a, an edge is added between a blue node and the green one to increase the overall clustering coefficient, while at step 4b, an edge is added between an orange node and the green one thus decreasing the clustering coefficient. Step N shows how the network might look like after a couple of iterations with a new green node that has to be attached either to increase or decrease the clustering coefficient. (Color online)

probability P leads to an increase in the CC. The results for the WS model are identical to those originally reported by Watts & Strogatz, with here $N = 1,000$ and an average degree $\langle k \rangle = 4$.

Using the MHK model provides us with a very good testbed to analyze network properties since it is possible to keep the number of agents and number of edges constant while changing other properties of the network—e.g. CC, SP, degree distribution, etc. The CC can be readily and continuously tuned within the interval $[0, 0.7]$, simply by varying the parameter P in the unit interval. The networks have an average degree $\langle k \rangle$ tending towards 4 as the number of nodes N increases. Indeed, the average degree of a network grown using the MHK model reads

$$\langle k \rangle = \frac{8 + 4(N-4)}{N}. \tag{B 1}$$

It is therefore impossible to control the variations of the average degree as can be done using the WS model. In the particular case whereby the number of swarming agents is $N = 1,000$, the average degree is $\langle k \rangle = 3.992$. To allow for a quantitative comparison of the MHK and WS models, all networks generated using the WS model have therefore been chosen to have an average degree of 4. As can be seen in Figure B3, the MHK model is able to produce networks with fat-tailed-like degree distributions distinct from the homogeneous distribution prototypical of the WS model, while having almost the same average degree. However, it is important highlighting here that the range of values for k is fairly limited ($\max(k) \sim 20$) owing to the relatively small size of the swarm (and consequently of the SSN) and to the

https://doi.org/10.1017/nws.2016.5 Published online by Cambridge University Press

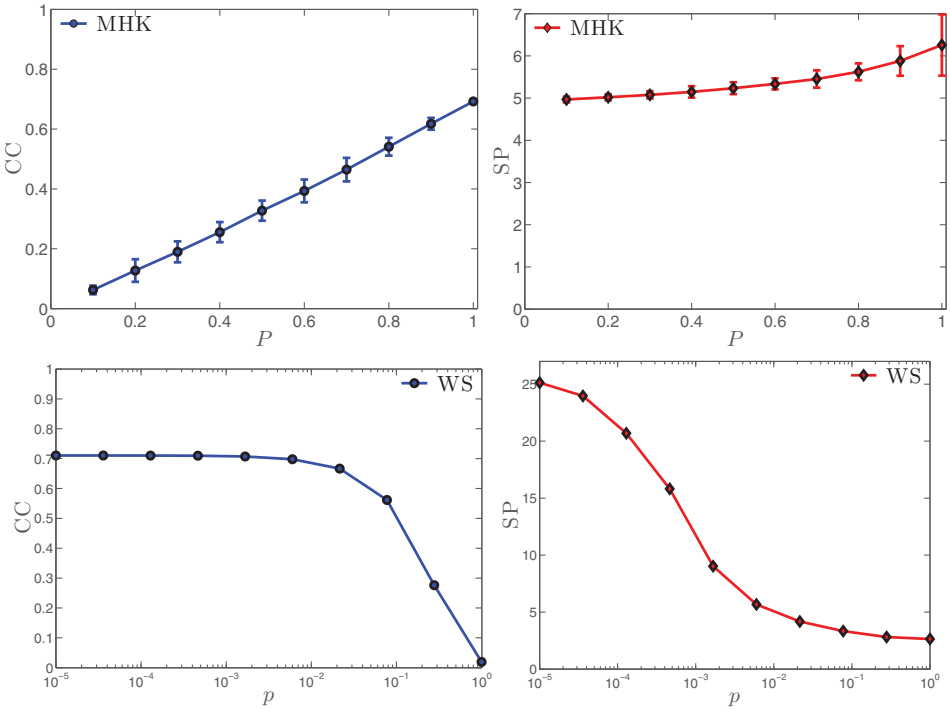

Fig. B2. Left: Clustering coefficient, CC, and Right: Shortest connecting path, SP, for 10 values of the probability P (resp. p) in the unit interval; P (resp. p) being the control parameter of the MHK (resp. WS) model. Top row: for the MHK model, each data point is obtained by averaging over a statistically ample enough sample comprising 50 networks, each having $N = 1,000$ nodes and $E = 3,992$ edges. The error bars represent the standard deviations to the average values. Bottom row: for the WS model, each data point is obtained by averaging over 50 networks, each having $N = 1,000$ nodes and an average degree $\langle k \rangle = 4$. (Color online)

limited number of connections—i.e. small average degree—that can be established between interacting agents. Note that this small range of values for k combined with the observed distributions in Figure B3 guarantee a fairly small variance of the degree about its average value.

It is often argued that the degree distribution is key to many global outcomes, such as stability (Olfati-Saber *et al.*, 2007), consensus reaching (Chung, 1996), and controllability (Liu *et al.*, 2011, 2012; Komareji & Bouffanais, 2013a,b). There is no doubt that the significant difference in degree distribution of the MHK and WS models highlights a fundamental difference in the underlying structure of the respective networks.

B.2 Directed networks

The flow of information has been shown to be directed in many kinds of natural and artificial multi-agent networked systems: bird flocks, fish schools, and wireless sensory networks to name a few (Olfati-Saber, 2006). It is therefore essential to extend our investigation to cases involving directed networks. Before going any further with our analysis of directed SSNs, it is worth stressing some known and yet

https://doi.org/10.1017/nws.2016.5 Published online by Cambridge University Press

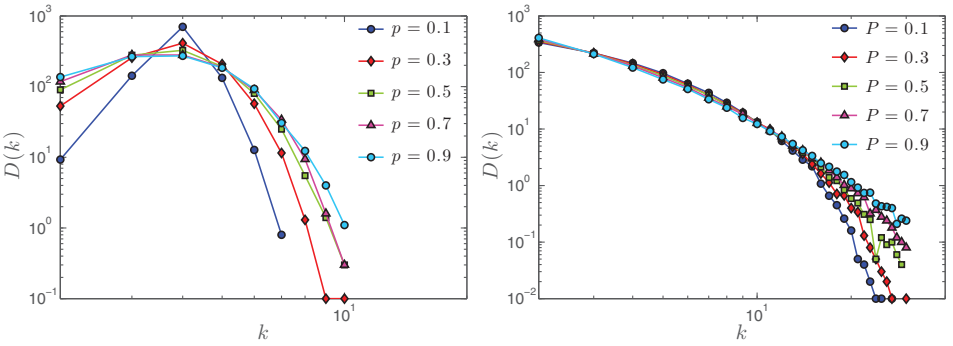

Fig. B3. Left: degree distribution, $D(k)$, for the WS model for five different values of the order parameter p. Right: degree distribution, $D(k)$, for the MHK model for five different values of the control parameter P. Both degree distributions are obtained from networks having a total of $N = 1{,}000$ nodes and an average degree $\langle k \rangle = 4$ (resp. $\langle k \rangle = 3.992$) for the WS (resp. MHK) model and through an averaging over 100 samples for each value of p (resp. P). (Color online)

important differences between directed and undirected networks. When considering undirected networks, the CC is defined using triangles made of undirected edges in the network (Barrat *et al.*, 2008). However, in the case of directed networks, four distinct types of CCs can be considered depending on how triangles are formed out of directed edges (Fagiolo, 2007). Following the definitions and terminology of Fagiolo (2007), we consider the following definition of the CC out at node i:

$$\mathrm{CC}_{\mathrm{out},i} = \frac{(A^2 A^T)_{ii}}{d_{\mathrm{out},i}(d_{\mathrm{out},i} - 1)}, \tag{B 2}$$

where $\mathbf{A}$ is the adjacency matrix and $\mathbf{D}_{\mathrm{out}} = \mathrm{diag}(d_{\mathrm{out},i})$ is the outdegree matrix. The overall (network-wide) CC out is then obtained by averaging over the nodes:

$$\mathrm{CC}_{\mathrm{out}} = \frac{1}{N} \sum_{i=1}^{N} \mathrm{CC}_{\mathrm{out},i}. \tag{B 3}$$

We use this definition throughout this paper as neighbors of each node in our directed networks are pointed at with outward edges, thus being compatible with what has already been applied in Olfati-Saber *et al.* (2007) and Komareji & Bouffanais (2013b). Moreover, the degree of a node also needs to be specified in a different way—for undirected networks the in- and out-degree are identical which is generally not the case with directed networks. Here, it is only the in-degree distribution that is examined since the out-degree is constant and equal for all nodes given that our model is based on the k-nearest neighbor rule to represent the topological distance. With these differences in mind, we propose a MTNI model that is based on a directed signaling network. Similarly, to the case based on undirected networks in the framework of the MHK and WS models, we aim at investigating the influence of some adequately controlled network properties on swarm dynamics in terms of consensus reaching.

The MTNI model is a one-parameter stochastic model devised to allow for the tuning of the CC (out) by changing the probability $\mathscr{P}$ of choosing a neighbor at random versus a nearest neighbor in the topological sense. Specifically, at the core,

https://doi.org/10.1017/nws.2016.5 Published online by Cambridge University Press

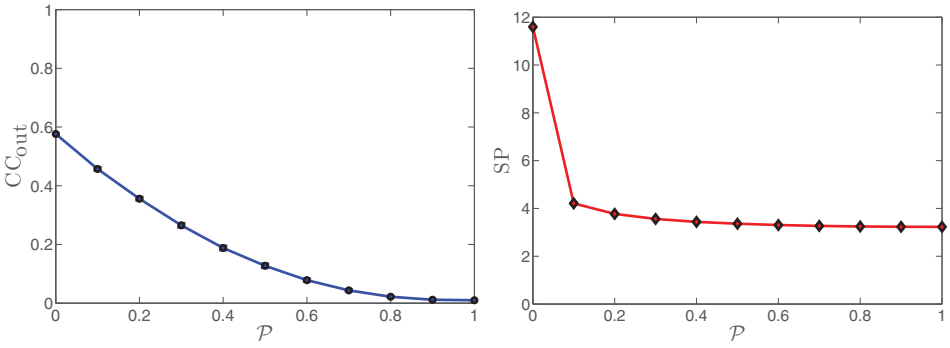

Fig. B4. Left: Out clustering coefficient, CC_{out}, and Right: Shortest connecting path, SP, for 10 evenly distributed values of the probability $\mathscr{P}$ in the unit interval; $\mathscr{P}$ being the control parameter of the MTNI model. Each data point is obtained by averaging over a statistically ample enough sample comprising 50 networks, each having $N = 1,000$ nodes and $k = 10$ neighbors, i.e. a fixed out-degree of 10. (Color online)

the MTNI model is based on the topological neighborhood distance observed in flocks of starlings (Ballerini *et al.*, 2008). The MTNI model can be split up into two parts, the TNI model and a random rewiring. The model works by first randomly distributing the nodes on a 2D plane. Each node is then given a fixed number k of neighbors to point at, where each neighbor with probability $1 - \mathscr{P}$ are picked from the set of k-nearest neighbors based on the smallest Euclidean separation distance. In the extreme case where $\mathscr{P}$ is 0, the model generates k-nearest neighbor networks Komareji & Bouffanais (2013b). Conversely, when $\mathscr{P} = 1$, the SSN is a pure random directed regular network with a fixed out-degree k.

Interestingly, a one-to-one relationship between the CC and the control parameter $\mathscr{P}$ is also uncovered for the MTNI model, similarly to what was previously obtained with the WS and MHK models. The SP decreases monotonously with $\mathscr{P}$ with extremely variations above $\mathscr{P} = 0.2$. This can easily be seen in Figure B4. This first result is of importance as it proves that we have full control over the CC through the tuning of $\mathscr{P}$. However, the upper limit on CC_{out} is approximately 0.6 and corresponds to $\mathscr{P} = 0$, i.e. for the pure TNI model. This result is in total agreement with those reported in Komareji & Bouffanais (2013b). The MTNI model therefore has the advantage of producing networks where the agents have a constant out-degree and constant average in-degree, while CC_{out} can continuously be changed within the interval $[0, 0.6]$. The impossibility to generate CC_{out} beyond the upper limit of 0.6 did not prove to be an issue in our study since networks possessing high CCs tend to be quite ineffective at global consensus reaching. On the contrary, small values of CC_{out} are sought when the emphasis is put on the effectiveness of achieving global consensus.

After this study of CC_{out}, we now turn to the in-degree distributions associated with the MTNI model with varying control parameter $\mathscr{P}$. The case $\mathscr{P} = 1$ is straightforward as it is a purely random network, we expect a normal degree distribution centered about the average degree, which is equal to the constant out-degree. At the other end of the unit interval, the case $\mathscr{P} = 0$ corresponds to the pure TNI model, which was shown to lead to a Poissonian-like distribution (Komareji

https://doi.org/10.1017/nws.2016.5 Published online by Cambridge University Press

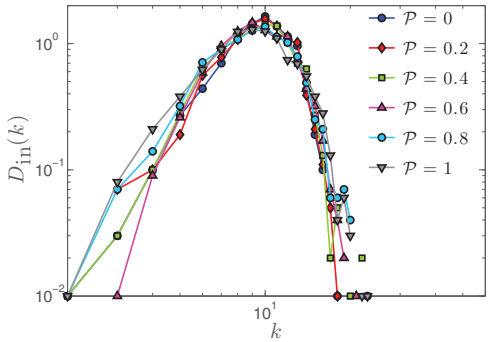

Fig. B5. In-degree distributions, $D_{\rm in}(k)$ for directed networks generated with the MTNI model with the out-degree set to $k = 10$. Six values of the control parameter $\mathscr{P}$, evenly distributed within the unit interval, were considered. All six in-degree distributions are associated with networks having $N = 1,000$ nodes. (Color online)

& Bouffanais, 2013b). In the present case, we consider the particular case $k = 10$ and with such a relatively large out-degree, the Poissonian-like distribution reduces to an almost Gaussian one. Four other values of $\mathscr{P}$ have been considered and the associated in-degree distributions are shown in Figure B5. One observes that with the out-degree $k = 10$, the MTNI model produces networks with practically Gaussian distribution for all values of the control parameter $\mathscr{P}$.

Appendix C: List of abbreviations and acronyms

Symbol/Acronym	Definition
SSN	Swarm signaling network
SPP	Self-propelled particles
CC	Clustering coefficient
SP	Shortest connecting path
WS	Watts & Strogatz model
MHK	Modified Holme & Kim model
MTNI	Modified topological neighborhood of interaction
λ_2	Algebraic connectivity
N	Number of network nodes
E	Number of network edges
$\langle k \rangle$	Average degree
$D(k)$	Degree distribution
φ	Order parameter of the swarm
ℓ	Dimension of the square domain
$\rho = N/\ell^2$	Swarm density

https://doi.org/10.1017/nws.2016.5 Published online by Cambridge University Press